The Developmental Process of Xylem Embolisms in Pine Wilt Disease Monitored by Multipoint Imaging Using Compact Magnetic Resonance Imaging[1][OA]

Toshihiro Umebayashi*, Kenji Fukuda, Tomoyuki Haishi, Ryo Sotooka, Sule Zuhair, and Kyoichi Otsuki

Laboratory of Evaluation of Natural Environment, Institute of Environmental Studies, Graduate School of Frontier Sciences, The University of Tokyo, Kashiwa 277–8563, Japan (T.U., K.F., R.S., S.Z.); Research Team for Detection of Plant Pathogens and Nematodes, National Agricultural Research Center, National Agriculture and Food Research Organization, Tsukuba 305–8666, Japan (T.U.); MRTechnology, Inc., Tsukuba 305–0047, Japan (T.H.); and Kasuya Research Forest, Graduate School of Agriculture, Kyushu University, Sasaguri 811–2415, Japan (K.O.)

In pine wilt disease (PWD), embolized tracheids arise after virulent pine wood nematodes (PWN), *Bursaphelenchus xylophilus*, invade the resin canal of pine tree; infected pine trees finally die from significant loss of xylem water conduction. We used a compact magnetic resonance imaging system with a U-shaped radio frequency (rf) probe coil to reveal the developmental process of the xylem dysfunction in PWD. Multiple cross-sectional slices along the stem axis were acquired to periodically monitor the total water distribution in each 1-year-old main stem of two 3-year-old Japanese black pines (*Pinus thunbergii*) after inoculation of PWN. During the development of PWD, a mass of embolized tracheids around the inoculation site rapidly enlarged in all directions. This phenomenon occurred before the significant decrease of water potential. Some patch-like embolisms were observed at all monitoring positions during the experimental period. Patchy embolisms in a cross-section did not expand, but the number of patches increased as time passed. When the significant decrease of water potential occurred, the xylem dysfunctional rate near the inoculation point exceeded 70%. Finally, almost the whole area of xylem was abruptly embolized in all cross-sections along the stem. This phenomenon occurred just after water conduction was mostly blocked in one of the cross-sections. Thus, it appears that the simultaneous expansion of embolized conduit clusters may be required to induce a large-scale embolism across the functional xylem. Consequently, xylem dysfunction in infected trees may be closely related to both the distribution and the number of PWN in the pine stem.

The xylem sap of woody plants generally moves due to negative pressure; thus, the water column is vulnerable to cavitation. In the field environment, water stress (Sperry and Tyree, 1988, 1990; Brodribb and Cochard, 2009) and freezing stress (Sperry and Sullivan, 1992; Sperry, 1993; Pittermann and Sperry, 2006) are the two major causes of cavitation that cause a xylem conduit (vessel or tracheid) to lose its water-conducting function. Cavitation is caused by the entry of air into a water-filled conduit usually through the pit membrane, and if this air expands, the conduit is embolized (i.e. completely air filled; Utsumi et al., 1999, 2003; Ball et al., 2006). Generally, woody plants have excellent adaptable water-conducting systems that enable them to survive through the seasonal stresses of the regional climates in which they grow (Sperry et al., 1994; Maherali et al., 2004; Jacobsen et al., 2007). However, some pathogens (e.g. fungi and bacteria) can invade the xylem, seriously damaging the water-conducting pathway. In some wilt diseases (e.g. Dutch elm disease, oak wilt, and chestnut blight), sudden death of the host trees is caused by massive blockage of the xylem conduit (Smith, 1970; Tyree and Zimmermann, 2002; Agrios, 2005). To clarify the mechanism of xylem dysfunctions in these wilt diseases, it is necessary to determine the relationship between the developmental process of xylem embolisms and the distribution of pathogens in the xylem.

Pine wilt disease (PWD) is a unique disease of pine trees that is caused by a nematode species called the pine wood nematode (PWN), *Bursaphelenchus xylophilus* (Tokushige and Kiyohara, 1969; Kiyohara and Tokushige, 1971; Tamura, 1983). In living pine trees, PWN rarely invade the xylem conduits but distribute in the cortical and xylem resin canals (Mamiya, 1975; Ichihara et al., 2000). They can then move through the resin canals to reach almost all parts of the stem and branches fairly rapidly (Hashimoto and Kiyohara, 1973; Kuroda and Ito, 1992; Kuroda, 2008). In infected pine trees, both virulent PWN (Sasaki et al., 1984; Tamura et al., 1988;

[1] This work was supported by KAKENHI (Grant-in-Aid for Scientific Research [B] 20380086).

* Corresponding author; e-mail umebayashi@nenv.k.u-tokyo.ac.jp.

The author responsible for distribution of materials integral to the findings presented in this article in accordance with the policy described in the Instructions for Authors (www. plantphysiol.org) is: Toshihiro Umebayashi (umebayashi@nenv.k.u-tokyo.ac.jp).

[OA] Open Access articles can be viewed online without a subscription.

www.plantphysiol.org/cgi/doi/10.1104/pp.110.170282

Kuroda, 1991) and avirulent PWN (Fukuda et al., 1992b; Ikeda and Kiyohara, 1995; Fukuda, 1997) cause some localized embolisms in the xylem. The virulent PWN then significantly multiply in the pine stem (Mamiya, 1975; Kiyohara and Suzuki, 1978; Kiyohara and Bolla, 1990), and the leaf-water potential abruptly decreases, inducing death (Hashimoto, 1976; Ikeda et al., 1990; Fukuda et al., 1992a). At this moment, a large number of tracheids are abruptly embolized in the pine xylem until the water-conducting pathway loses its function completely (Ikeda and Suzaki, 1984; Ikeda and Kiyohara, 1995). This phenomenon has been referred to as "runaway embolism" (Ikeda, 1996; Fukuda et al., 2007). To clarify the developmental process of embolisms, some researchers have tried to separate the sudden development of symptoms in the advanced stages from the successive symptoms of the early stage (Fukuda et al., 1992a, 2007; Ikeda, 1996). It has also been hypothesized that abrupt cavitation development is caused by the alteration of metabolism and death of living cells in the xylem (Ikeda and Suzaki, 1984; Nobuchi et al., 1984; Kuroda, 1991). Nevertheless, this does not completely explain the mechanisms of two specific symptoms: embolisms observed as localized patches in the early stage, and abrupt runaway embolism enlarging to occupy the total xylem area in the advanced stage. Observation of the increasing and enlarging processes of embolisms within an infected pine stem is necessary to understand these two different stages of this disease. It is almost impossible to illustrate the incremental process of the embolized tracheids without diachronic observations of the same sample.

Magnetic resonance imaging (MRI) is an effective tool for nondestructive monitoring of diachronic change in the xylem water status (Holbrook et al., 2001; Clearwater and Clark, 2003; Windt et al., 2006). Kuroda et al. (2006) introduced a technique involving three-dimensional imaging of embolized areas by a clinical MRI system, but the system was not designed to perform continual diachronic diagnoses in plant science. A compact MRI system for plants is the most practicable imaging instrument for monitoring the water-conducting pathway of plant xylem in detail (Utsuzawa et al., 2005; Fukuda et al., 2007; Van As, 2007). Utsuzawa et al. (2005) established a method for visualizing the diachronic change in xylem embolisms induced by PWN infection using a compact 1-Tesla MRI system. Fukuda et al. (2007) clearly divided the developmental process of xylem embolism into the increase of some patch embolisms in the early stage and the rapid enlargement of embolisms in the advanced stage, using both acoustic emission and high-resolution MR microimaging. Unfortunately, they could analyze only one thin cross-sectional image of the stem, because the solenoid radio frequency (rf) coil used as the detector probe was fixed around the pine stem at a certain height. Thus, they were unable to determine the vertical distribution of embolisms in the whole stem and its relationship to the pathogen distribution. This problem is crucial for determining the mechanism of abrupt occurrence of embolisms throughout the xylem (i.e. runaway embolism) in the advanced stage.

In this study, we nondestructively monitored the developmental process of xylem embolisms in the main stem of a pine seedling from inoculation to death. Two seedlings were fitted with a U-shaped rf coil that had an open front to take MR images of plant stems without winding rf coils around the stem (Fig. 1). This new MRI system enabled us to take cross-sectional MR images robustly at almost any vertical position on the main stem with a smaller diameter than the coil-opening gap, except for the branch node positions. Two three-year-old inoculated Japanese black pine seedlings (*Pinus thunbergii*) were used to clarify (1)

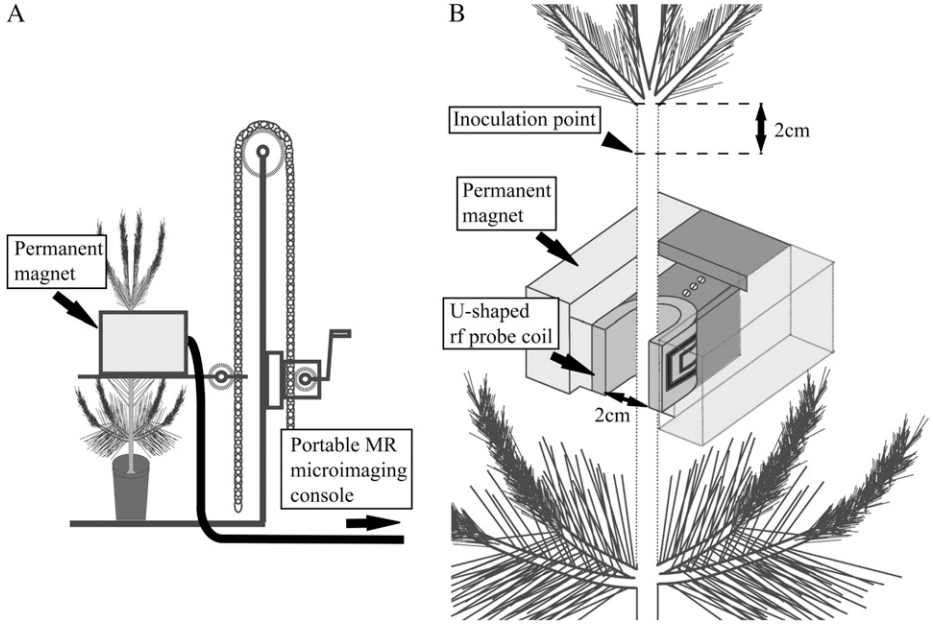

Figure 1. Compact MRI system with a C-shaped magnet loaded on a small hand lifter. A, The position of MR imaging, at the isocenter of the compact magnet, can be adjusted in the horizontal direction by the hand lifter. B, A U-shaped rf probe coil (2 cm inner opening gap) was installed in the air gap of the magnet so that its imaging position could be easily changed and detached from the sample trees.

the position where the first embolism occurs, (2) where and how new embolisms occur and how long they are in the axial direction of the stem, and (3) how embolisms expand in the radial, tangential, and axial directions of the stem. Based on these observations, we will discuss the relationship between water-conducting dysfunction and the activities of inoculated nematodes.

RESULTS

Effect of Wounding (Control)

In the cross-sectional MR images of pine stems, we could easily identify five different tissues: bark, cambium, the current year's annual ring, the previous year's annual ring, and pith. The cambium was the brightest zone (white); the pith was the center; and the xylem had the most characteristic contrast, with the previous-year latewood as a black ring.

Figure 2 presents MR images acquired from July 19 to September 1 in a control seedling inoculated with water. In the control, an inoculation wound cutting the edge of the current-year xylem was clearly observed in some cross-sections on July 19 (Fig. 2, arrowhead). No other changes were observed in any monitoring positions on July 19. The influence of the inoculation wound was observed from the uppermost position (0 cm) to the −2 cm position (Fig. 2, arrowhead). On August 4, the xylem water distribution did not change in cross-sections below −3 cm, although some wound-induced black areas (embolism) were observed in cross-sections from 0 to −2 cm. In these cross-sections, new white areas (callus and wound xylem) were laid by the neighboring cambium that had started to cover the wound (Fig. 2, small arrow). On September 1, the circumferential cambium had recovered in all of the positions except for −1 cm. A new cambium at −1 cm was engulfing the wound from both sides but had not connected to each other. In all cross-sections on September 1, an embolism of crescent shape was observed just beneath the newly formed xylem (Fig. 2, large arrows).

The base leaf-water potential hardly changed on any measurement date, and the lowest value was obtained on July 26 (−0.45 MPa).

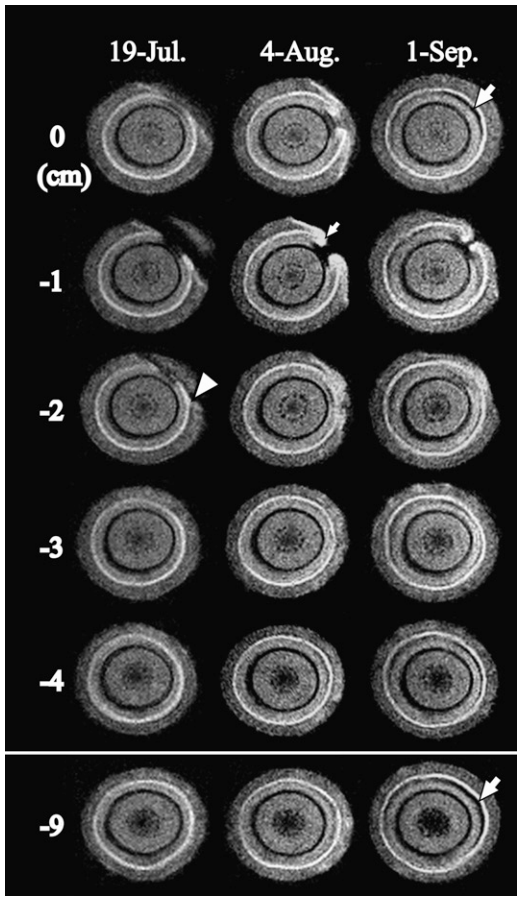

Figure 2. Cross-sectional MR images acquired from interval positions of 1 cm pitch within the monitoring region of the 1-year-old stem of the control tree after injection with distilled water. MRI parameters were as follows: repetition time = 500 ms, echo time = 19 ms, slice thickness in the axial direction = 1 mm. The arrowhead indicates injury by knife. The small arrow indicates newly made tissue that originated in the cambium. The large arrows indicate the embolism that was made within latewood of the injection site in the current year.

Monitoring of Embolism Development in the Stem (Ino-1)

In the first seedling inoculated with PWN (Ino-1), an inoculation wound was observed (Fig. 3, arrowheads), and an embolism of a fan-shaped mass reached from the wound to the pith in the two uppermost sections (0 and −1 cm) on July 15. The embolized area was larger at the upper positions (0 and −1 cm) than at the other positions, and some brightly colored areas (tracheids retaining water) were observed in the embolized mass at −2 cm. The embolized area in the section at −3 cm was smaller, and the one at −4 cm was restricted to the current-year xylem. No embolism was observed at or below −8 cm. At all positions, a thin crescent-shaped embolism was observed in the outermost xylem just beneath the cambium (Fig. 3, arrow a).

On and after July 15, the embolized area expanded from the inoculated side in both tangential and axial directions. On July 23, the embolized area covered about half of the total xylem area in the cross-sections at 0 and −1 cm. A smaller cross-section of the same embolized mass was observed at every lower position until July 27. By July 31, however, it was apparent that sudden, dramatic, and widespread expansion of embolism had occurred.

At the same time, patches or radial lines of embolism disconnected from a mass of an embolism were also observed in all cross-sections on July 19. These scattered patches hardly seemed to be expanding in the tangential direction, but they were increasing in number. On July 19, no patchy embolism was observed on the side opposite the inoculation wound at

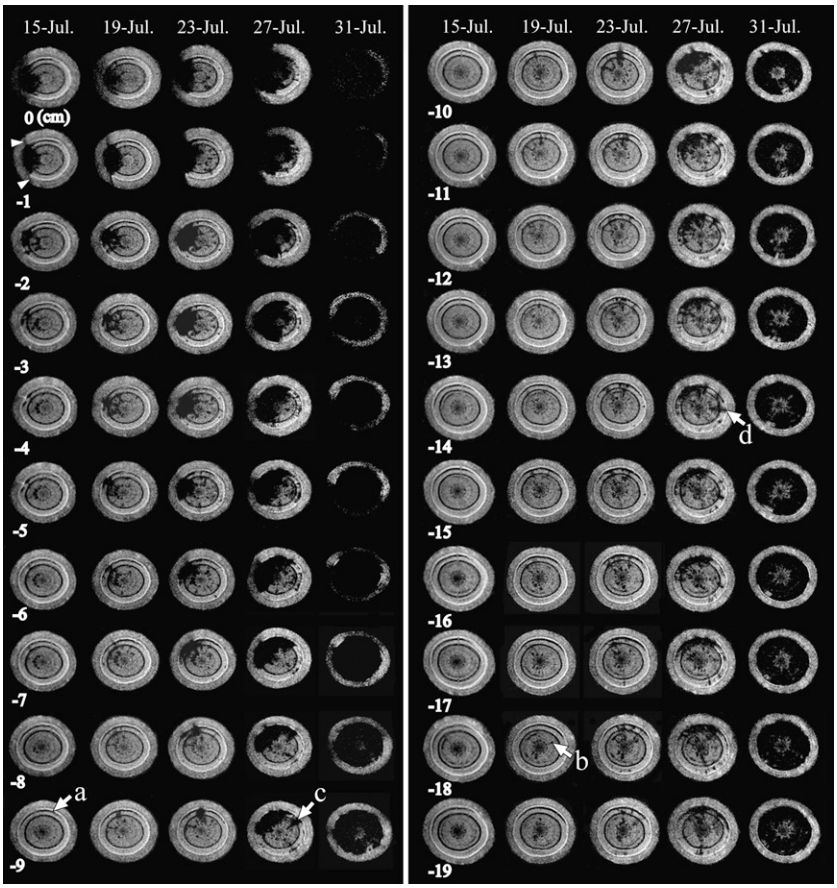

Figure 3. Cross-sectional MR images obtained from interval positions of 1 cm pitch within the monitoring region of a 1-year-old stem of Ino-1 after inoculation with PWN. MRI parameters were as follows: repetition time = 500 ms, echo time = 19 ms, slice thickness in the axial direction = 1 mm. The arrowheads indicate injury by knife. Arrow a indicates an embolism that was made within the xylem in the current year. Arrow b indicates scattered embolisms. Arrow c indicates a separate massed embolism. Arrow d indicates the new occurrence of a massed embolism.

0 cm, while at −18 cm, the embolism was clearly observed (Fig. 3, arrow b). On July 23, embolisms were also observed on the side opposite the inoculation. The increasing rate of embolisms in cross-sections clearly differed among the positions observed by MRI. The embolisms tended to increase most rapidly in cross-sections near the inoculation point, and the area remained smaller in more distant positions (Fig. 4A).

We defined this radially expanding embolized mass in xylem, which finally reaches from cambium to pith, as a "massed embolism," and we defined embolism of the scattered patches as "scattered embolism." Repeated measurements from multipoint MRI monitoring on the same seedling indicated that the massed embolism expanded in all directions (radially, tangentially, and longitudinally). This massed embolism started to expand from the inoculation position to −5 cm on July 19. On July 23, the massed embolism extended 2 cm further in the lower direction (to −7 cm), and by July 27, it covered half of the total xylem area or more in the upper cross-sections; vertically, it had reached the lowermost monitoring position by swallowing some scattered embolisms. On July 27, another sagittate massed embolism appeared in the cross-section at −9 cm (Fig. 3, arrow c). This embolism was connected to the enlarged embolism body at −8 cm. In the lower positions, the new massed embolism became thinner and could hardly be distinguished at −11 cm, but it appeared again at −14 cm (Fig. 3, arrow d).

The total embolized area in a cross-section reached 41.1% of the total xylem area at 0 cm by July 23 (Fig. 4A), and the most embolized area of all monitoring positions reached 78.6% on July 27 (Fig. 4B). Regardless of such an increase in the embolized area, a slight increase in the base leaf-water potential (−0.7 MPa) was still observed. When the total xylem area at 0 cm was embolized (August 31; 100%), the other positions indicated a relative embolized area of more than 90%, and the water potential dropped dramatically (−1.8 MPa).

From July 19 to 27, at all positions, the water loss in both the cambial zone and the phloem was observed in more restricted spaces than the massed embolisms in the xylem. On July 31, cambium and phloem at the uppermost positions between 0 and −2 cm turned black (dried). Positions below −8 cm still exhibited no change in cambium or phloem.

Precise Monitoring of Embolism Near the Inoculation Position (Ino-2)

Figure 5 presents MR images of Ino-2 from August 22 to October 2. Before inoculation, a thin crescent-shaped embolism was observed between the cambium and the current-year xylem at all positions (Fig. 5A,

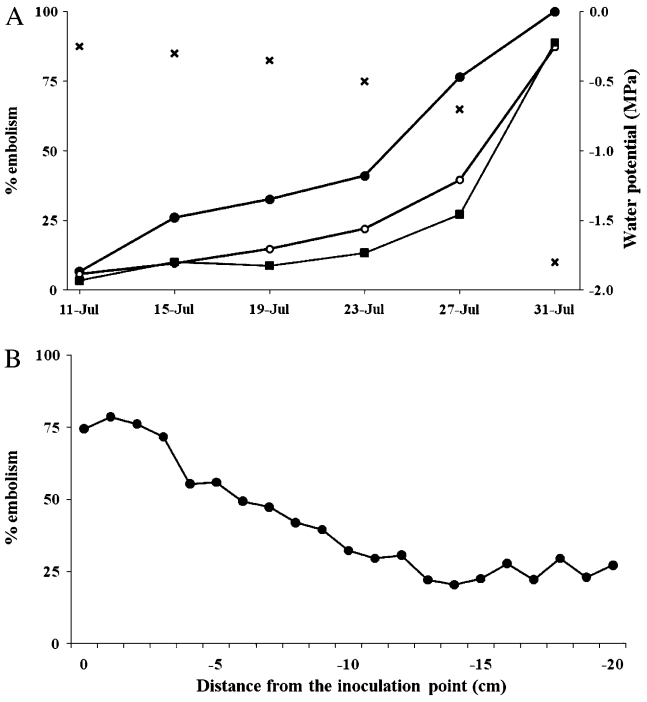

Figure 4. Quantitative evaluations of embolisms of Ino-1 by MRI. A, The relationship between the percentages of xylem embolism in 0 cm (black circles), −10 cm (white circles), and −20 cm (black squares) and base leaf-water potential (crosses; MPa) on each monitoring day. B, The percentage of xylem embolism of all MRI positions on July 27.

arrowhead). On August 28, the effect of wounding was not observed even just beneath the wound (0.0 mm). New thin layers of embolisms developed from the current-year xylem neighboring the cambium inward at −5.0 to −10.0 mm (Fig. 5A, arrow). This embolism neighboring the cambium actively expanded in all directions, and the first massed embolism was confirmed between −5.0 and −7.5 mm. On September 17, this massed embolism reached the full length of vertical observation positions. The cross-sectional area of the massed embolism at −5.0 to −7.5 mm expanded faster than at other positions until September 30. On October 2, the massed embolism covered almost all the xylem at all positions.

Some scattered embolisms were observed in all cross-sections on September 4. Some were thin and longitudinally straight, since they were located at nearly the same position in different cross-sections (Fig. 5B, arrowheads). Some embolisms appeared as a radial line in cross-sections (Fig. 5B, arrow). More and more scattered embolisms appeared at all positions as the disease progressed, although the embolism of each scattered patch did not tend to expand like the massed embolism.

At −5.0 mm, the ratio of embolized area in the xylem reached 55.6% on September 22, and the base water potential was below −0.5 MPa at that time. When the area at this position reached 71.0% (September 26), the base leaf-water potential significantly decreased (−1.2 MPa). On October 2, the embolized mass covered more than 90% and the water potential reached –1.8 MPa.

The MR images of the cambium and phloem on the inoculated side slowly became black from −2.5 to −10.0 mm, but they were almost unchanged at the opposite side throughout the experiment period at all positions.

Anatomical measurements of xylem of Ino-2 showed that the tracheid length of the current-year xylem was 1.07 ± 0.17 mm (mean ± SD), that of the previous-year earlywood was 1.01 ± 0.17 mm, and that of the previous-year latewood in the 1-year-old stem was 1.15 ± 0.15 mm.

DISCUSSION

To clarify the developmental process of xylem embolism in PWD, the water distribution of 1-year-old main stems in inoculated seedlings was observed non-destructively by a new technique of multiple cross-sectional MR imaging using a U-shaped rf coil. In seedling Ino-2, the imaging interval was 2.5 mm, and one filming thickness was 1.0 mm; therefore, we overlooked the 1.5 mm length between the monitored positions. Since the tracheid length was 1.0 mm, a maximum of two tracheids could have been overlooked. Thus, our observations were assumed to be sufficient to permit analysis of the three-dimensional expansion of xylem water-conducting dysfunction.

After inoculation of PWN, the pattern of occurrence and development of embolisms was common between the two seedlings. One week after inoculation, new embolism of a mass in xylem (i.e. massed embolism) was observed near the inoculation wound, and it expanded from the inoculation site in all directions (Figs. 3 and 5A). Fukuda et al. (2007) indicated that the occurrence of embolisms was closely correlated to the occurrence of acoustic emission, and the increase in acoustic emission events in current-year shoots (near the inoculation point) was observed earlier than that at the stem base. For each term of MRI monitoring, the relative embolized area in a cross-section near the inoculation point increased more rapidly than at the lower positions (Fig. 4A), and the relative area of embolisms in a cross-section was highest at the uppermost (inoculated) positions and decreased at the lower positions (Fig. 4B). Thus, massed embolism was clearly caused by nematodes colonizing the tissues around the inoculation wound. Another embolism type, scattered embolism, appeared randomly after the appearance of the massed embolism around the inoculation wound. The scattered embolisms had two shapes: longitudinal and radial (Fig. 5B). The appearance of the two different types may depend on the relationship between nematode activity and the direction of the resin canal or parenchyma tissue.

Utsuzawa et al. (2005) observed scattered embolisms before the appearance of a massed embolism by

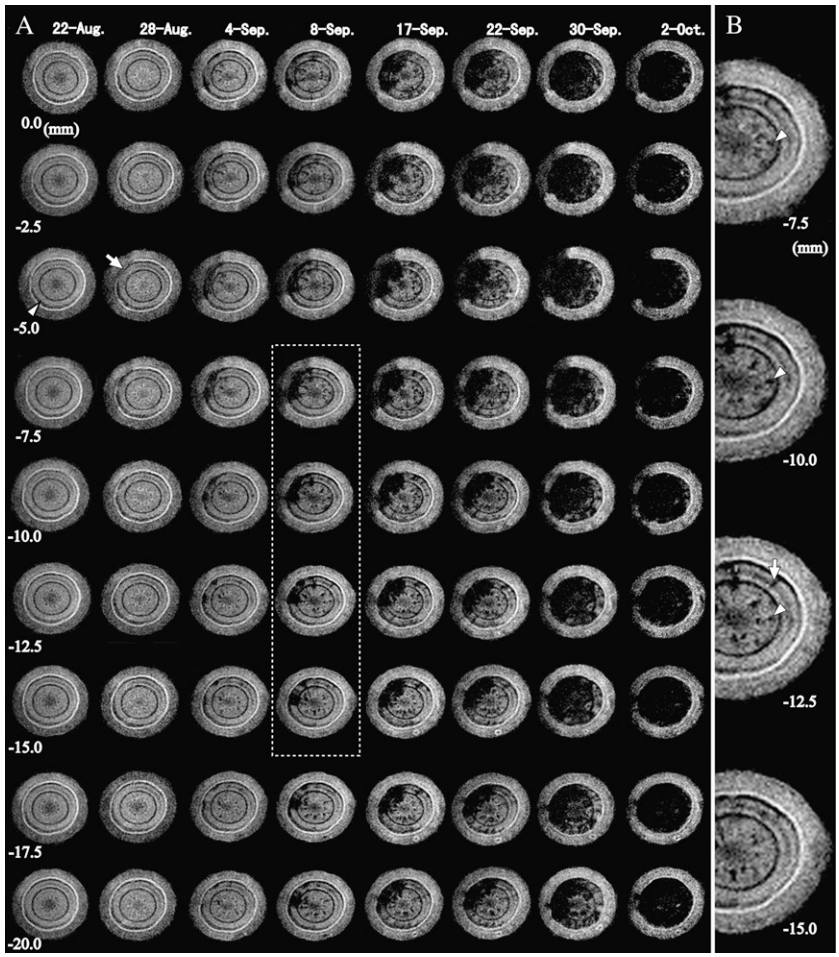

Figure 5. Cross-sectional MR images obtained from interval positions of 2.5 mm pitch within the monitoring region of a 1-year-old stem of Ino-2 after inoculation with PWN. MRI parameters were as follows: repetition time = 500 ms, echo time = 19 ms, slice thickness in the axial direction = 1 mm. A, Global development of xylem dysfunction in the monitoring region. The arrowhead indicates the embolism that was made within latewood in the current year. The arrow indicates the starting region of the massed embolism. The dotted grid denotes the extensional region in B. B, Magnification of the right half of the MR images between –7.5 and –15.0 mm on September 8. The scattered embolisms were two different types: longitudinal (arrowheads) and radial (arrow).

diachronic monitoring, possibly because the monitoring position was distant from the inoculation point. In this study, most of the scattered embolisms did not expand in volume but increased in number as the disease progressed. For Ino-1, on July 27, the relative area of embolized xylem at −14 cm was the smallest of all monitoring positions (20.4%), and the value between −14 cm and −20 cm fluctuated between 20.4% and 29.5%. This result indicates that the xylem dysfunction in PWD does not develop in a simple way, such as gradual spreading from the inoculation point. No simple decreasing trend occurred in the total embolized area in cross-sections from the inoculation point because of varied components (e.g. occurrence of randomly scattered embolisms, new massed embolisms, and branched embolisms from the massed embolism).

To our knowledge, these two different developmental processes of embolism could be clearly distinguished for the first time by our multipoint imaging, which enabled reconstructing the three-dimensional structure and distribution of embolism in PWD.

We analyzed how the two different embolism developments relate to the wilting mechanism in PWD. For several days after infection, most of the inoculated nematodes remain near the inoculation point, and only a small part of the PWN population can disperse into the other parts of the stem through resin canals (Mamiya, 1980, 1985, 1990). In this phase, xylem embolism and tracheid occlusion occur (Kuroda, 1991). Because the nematode itself rarely enters into the tracheids of living pine (Ichihara et al., 2000), some researchers have attributed the abrupt increase in embolized tracheids to modification of the surface tension of xylem sap (Ikeda and Kiyohara, 1995), cellulase production of PWN (Odani et al., 1985), released oily substance occluding the tracheid lumen and pit membrane (Nobuchi et al., 1984; Hara and Futai, 2001), and abnormal leaks of oleoresin from resin canals (Sasaki et al., 1984). In addition, some researchers have suggested that some compounds, such as terpenoids released from parenchyma cells (Kuroda, 1989, 1991) and ethylene produced in xylem (Fukuda, 1997), can induce xylem embolism, based on the results of artificial injection of these compounds into the stem. In coniferous species, a significant increase of the cavitation event by water stress is usually synchronized with a drastic decrease of water potential (Brodribb and Cochard, 2009). However, the increase of the event in the PWD plant was induced

within the normal water potential of a non-water-stress condition (Fig. 4A). In woody plants, lowering sap surface tension by adding surfactants increases xylem vulnerability: cavitation occurs at higher water potential (Cochard et al., 2009). Unless PWN produce a mechanical defect of earlywood tracheids, it is likely that the xylem embolism in PWD is introduced by a lowered surface tension of xylem sap, caused by PWN. Thus, the incidence of embolisms of PWD should be related to the nematode population in the same position.

We could not count the nematode population on each monitoring date, since nematode isolation is destructive. However, we can assume that both the occurrence and the expansion of massed embolisms at the inoculation position were induced by the greater nematode population there. In contrast, scattered embolisms occurred randomly throughout the stem and increased in number, but they did not expand in either radial or tangential direction (Figs. 3 and 5A). Moreover, the scattered embolisms had two shapes along the axial and radial resin canals. This type of embolism may be caused by nematodes moving through the resin canals in the stem (Kuroda and Ito, 1992). In addition, the size variation of the scattered embolisms could be explained by not only the variation in the number of nematodes in the resin canals but also physiological factors such as xylem tension or the volume of cavitation-inducing substances released from the nematodes or from xylem living cells by nematode activities. Thus, we assume that both the occurrence and expansion of the two different embolism types (massed and scattered embolisms) are induced by the different actions of migrating and settled nematode populations. Some of the nematode population migrating from the inoculation point settles in certain places, inducing new massed embolisms, and their multiplication might be related to the occurrence of embolisms. Previous studies on xylem water dysfunction in PWD (summarized by Kuroda, 2008) did not distinguish the two embolism types; however, their two different mechanisms of embolism should be considered hereafter. This study suggested that attacks of a lumped nematode population are necessary to induce massed embolism, since massed embolisms expanded from the inoculation position where the nematode population was the largest. Thus, future studies should investigate the mechanism of the expansion of a massed embolism in relation to the size of the local nematode population.

Our results demonstrated that an abrupt embolism covered almost all conducting tracheids throughout the 1-year-old stem in a short time (less than 3 or 4 d), although neither the expansion of a massed embolism nor an increase in the number of scattered embolisms fully occupied the whole xylem area at any monitoring position at the time of the last observation, just before the abrupt embolism. It has been hypothesized that runaway embolisms occur at the advanced stage of this disease, inducing an abrupt decrease in leaf-water potential (Ikeda, 1996; Fukuda et al., 2007). In our study, a drastic increase was clearly observed between July 27 and July 31 of Ino-1 (Fig. 4A). On July 27, the relative area of the embolized region in cross-sections varied from 25% to 80%, but the occurrence rate on July 31 exceeded 90% at all monitoring positions. The abrupt occurrence of embolisms in the whole xylem area may be runaway embolism.

In addition, our MRI data clearly indicated the existence of embolisms that were not caused by nematode infection. Of all the samples, only latewood in the previous-year annual ring had already been embolized before the inoculation, and a different kind of thin crescent-shaped embolism from the massed embolism was also observed from a portion of the outermost xylem neighboring the cambium (Figs. 3, arrow a, and 5A, arrowhead). In Ino-2, a massed embolism was initiated from the current-year xylem neighboring the cambium. In natural conditions, most tracheids in the transition zone from earlywood to latewood of conifers are more susceptible to cavitation by water stress in *Pinus* species (Utsumi et al., 2003). These results confirm the susceptibility of the transition zone to cavitation. Previous studies suggest that the death of phloem and cambium is also an important symptom that occurs at the same time as embolisms in the current-year xylem (Fukuda et al., 1992b; Fukuda, 1997). In our observations, the phloem and cambium did not dry up (die) until runaway embolism occurred (Figs. 3 and 5A). Therefore, the death of cambium and phloem is not the cause of runaway embolisms in the outermost xylem in these pine stems; rather, it is their result.

In summary, we could systematically account for the pine death process in PWD through our novel technique using multiple slices with the U-shaped rf coil of a compact MRI. It is thought that the mass increase of embolized tracheids leads to pine seedling death, and massed embolisms seem to be caused by the nematode population's staying around the inoculation site. Clarification of the mechanism of massed embolism will be the key to the total resolution of this disease, and it will add new ideas on plant physiology when compared with "normal" cavitation in sound trees.

MATERIALS AND METHODS

Plant Materials and Nematode Inoculation

Three potted 3-year-old Japanese black pine (*Pinus thunbergii*) seedlings were grown at the Kashiwa campus of the University of Tokyo. The height of the seedlings ranged from 90 to 95 cm, and the diameter of the 1-year-old stem ranged from 1.1 to 1.2 cm. The PWN of a virulent isolate (S10) was reared on *Botrytis cinerea* grown on a potato dextrose agar plate at 25°C. Two seedlings were inoculated by injecting 0.03 mL of water suspended with 10,000 nematodes onto an oblique wound (0.5–1.0 cm depth) from the stem surface into the current-year xylem made with a razor blade 2 cm below the uppermost part of the 1-year-old main stem (Fig. 1B). Two seedlings (Ino-1 and Ino-2) were inoculated, one on July 11, 2008, and one on August 8, 2008. A control seedling was injected with distilled water in the same way on July 11, 2008. The base leaf-water potential was measured with a pressure

chamber (model 600; PMS) at predawn on each monitoring day using the MRI device.

Both seedlings were grown outside, except during the monitoring time (2–3 h in daytime). Every 2 to 3 d, 500 mL of water was supplied to the seedlings.

Multipoint Monitoring of Xylem-Water-Embolic Process on a 1-Year-Old Main Stem

We set 21 monitoring positions along the stem of two seedlings (Ino-1 and the control) at intervals of 1 cm below the inoculation point (0 cm). Before inoculation on July 11, three positions (top, middle, and bottom) were imaged by MRI. After inoculation, all 21 positions of Ino-1 were monitored at intervals of 4 d. The monitoring was terminated when the water-conducting xylem area, originally white in color, turned totally black (Utsuzawa et al., 2005). The control seedling was monitored after 4 d, 1 week, 1 month, and 2 months following the injection of water.

The MRI system used in this study consisted of a two-column permanent magnet with a field strength of 0.3 Tesla in a 6 cm air gap (Neomax) and a portable MR microimaging console (MRTechnology). A U-shaped rf probe coil (2 cm i.d.) was installed in the air gap of the magnet. The magnet was fixed to a hand lifter, allowing up-and-down movement of the magnet (Fig. 1A). Thus, during the monitoring period, multiple points on the stem could easily be scanned and the seedling could easily be detached from the MRI system (Fig. 1B). In this study, we used a T1-weighted spin-echo sequence with a repetition time (TR) of 500 ms and an echo time (TE) of 19 ms to observe the water distribution on a cross-section of a two-dimensional image matrix of 128×512 pixels (with an oversampled view field with isotropic voxel size). From previous studies, it is known that T1-weighted images with shorter TR are the most suitable for visualizing differentials between water-retaining xylem or living tissues and embolized xylem or dry necrotic tissues: the black areas indicate embolized tracheids in the stem during the water-conducting dysfunction in a pine monitored under T1-weighted conditions (Utsuzawa et al., 2005; Kuroda et al., 2006).

Precise Monitoring of Embolisms Near the Inoculation Position and Measurement of Tracheid Length

Before inoculation, we set nine monitoring positions along the stem of seedling Ino-2 at intervals of 2.5 mm, with all positions imaged using MRI. After inoculation, all positions were monitored at intervals of 2 to 4 d, with monitoring terminated when the whole xylem became black. The monitoring conditions and the TR and TE parameters were the same as for the other two seedlings (Ino-1 and control).

After we finished monitoring, a block 1 cm in length, including the inoculation position from the stem, was cut off to measure the tracheid length. The xylem block was separated into three parts: the current-year xylem and the earlywood and latewood of previous-year annual rings. Each xylem block was macerated at 60°C for 48 h with Schulz's solution (a 1:1 mixture of acetic acid and hydrogen peroxide), and the lengths of 50 tracheids from each sample were measured using a digital sight (DS-L2; Nikon) with a light microscope (Eclipse E800; Nikon).

Computation of the Embolized Area in Xylem in MR Images

All positions of Ino-1 and one position of Ino-2 were selected to evaluate the relative area of the xylem embolized area in cross-sectional MR images. All the images at these positions taken every imaging day were binarized by Photoshop (version 7.0; Adobe). The threshold level to divide black from white areas was determined as the value where the peak of all thermal noise outside the stem in the images was completely to the black side. The relative area in the xylem was computed using ImageJ (version 1.43u; National Institutes of Health).

ACKNOWLEDGMENTS

We thank Kazuma Togashi (MRTechnology) for support in constructing and testing the MRI apparatus.

Received December 5, 2010; accepted April 14, 2011; published April 19, 2011.

LITERATURE CITED

Agrios GN (2005) Plant Pathology, Ed 5. Elsevier Academic Press, San Diego

Ball MC, Canny MJ, Huang CX, Egerton JJG, Wolfe J (2006) Freeze/thaw-induced embolism depends on nadir temperature: the heterogeneous hydration hypothesis. Plant Cell Environ **29:** 729–745

Brodribb TJ, Cochard H (2009) Hydraulic failure defines the recovery and point of death in water-stressed conifers. Plant Physiol **149:** 575–584

Clearwater MJ, Clark CJ (2003) In vivo magnetic resonance imaging of xylem vessel contents in woody lianas. Plant Cell Environ **26:** 1205–1214

Cochard H, Hölttä T, Herbette S, Delzon S, Mencuccini M (2009) New insights into the mechanisms of water-stress-induced cavitation in conifers. Plant Physiol **151:** 949–954

Fukuda K (1997) Physiological process of the symptom development and resistance mechanism in pine wilt disease. J For Res **2:** 171–181

Fukuda K, Hogetsu T, Suzuki K (1992a) Photosynthesis and water status of pine-wood nematode-infected pine seedlings. J Jpn For Soc **74:** 1–8

Fukuda K, Hogetsu T, Suzuki K (1992b) Cavitation and cytological changes in xylem of pine seedlings inoculated with virulent and avirulent isolates of *Bursaphelenchus xylophilus* and *B. mucronatus*. J Jpn For Soc **74:** 289–299

Fukuda K, Utsuzawa S, Sakaue D (2007) Correlation between acoustic emission, water status and xylem embolism in pine wilt disease. Tree Physiol **27:** 969–976

Hara N, Futai K (2001) Histological changes in xylem parenchyma cells and the effects on tracheids of Japanese black pine inoculated with pine wood nematode, *Bursaphelenchus xylophilus*. J Jpn For Soc **83:** 285–289

Hashimoto H (1976) Pathological study of the pine wilting disease caused by *Bursaphelenchus lignicolus* under different conditions of watering. Trans Mtg Jpn For Soc **87:** 233–235

Hashimoto H, Kiyohara T (1973) Migration of the pine wood nematode in pine trees (III). Trans Annu Mtg Kyushu Br Jpn For Soc **26:** 330–332

Holbrook NM, Ahrens ET, Burns MJ, Zwieniecki MA (2001) In vivo observation of cavitation and embolism repair using magnetic resonance imaging. Plant Physiol **126:** 27–31

Ichihara Y, Fukuda K, Suzuki K (2000) Early symptom development and histological changes associated with migration of *Bursaphelenchus xylophilus* in seedling tissues of *Pinus thunbergii*. Plant Dis **84:** 675–680

Ikeda T (1996) Xylem dysfunction in *Bursaphelenchus xylophilus*-infected *Pinus thunbergii* in relation to xylem cavitation and water status. Ann Phytopath Soc Jpn **62:** 554–558

Ikeda T, Kiyohara T (1995) Water relations, xylem embolism and histological features of *Pinus thunbergii* inoculated with virulent or avirulent pine wood nematode, *Bursaphelenchus xylophilus*. J Exp Bot **46:** 441–449

Ikeda T, Kiyohara T, Kusunoki M (1990) Change in water status of *Pinus thunbergii* Parl. inoculated with species of *Bursaphelenchus*. J Nematol **22:** 132–135

Ikeda T, Suzaki T (1984) Influence of pine-wood nematodes on hydraulic conductivity and water status in *Pinus thunbergii*. J Jpn For Soc **66:** 412–420

Jacobsen AL, Pratt RB, Ewers FW, Davis SD (2007) Cavitation resistance among 26 chaparral species of southern California. Ecol Monogr **77:** 99–115

Kiyohara T, Bolla RI (1990) Pathogenic variability among populations of the pinewood nematode, *Bursaphelenchus xylophilus*. For Sci **36:** 1061–1076

Kiyohara T, Suzuki K (1978) Nematode population growth and disease development in the pine wilting disease. Eur J For Pathol **8:** 285–292

Kiyohara T, Tokushige Y (1971) Inoculation experiments of a nematode, *Bursaphelenchus* sp., onto pine trees. J Jpn For Soc **53:** 210–218

Kuroda K (1989) Terpenoids causing tracheid-cavitation in *Pinus thunbergii* infected by the pine wood nematode (*Bursaphelenchus xylophilus*). Ann Phytopath Soc Jpn **55:** 170–178

Kuroda K (1991) Mechanism of cavitation development in the pine wilt disease. Eur J For Pathol **21:** 82–89

Kuroda K (2008) Physiological incidences related to symptom development and wilting mechanism. *In* BG Zhao, K Futai, JR Sutherland, Y Takeuchi, eds, Pine Wilt Disease. Springer, Tokyo, pp 204–222

Kuroda K, Ito S (1992) Migration speed of pine wood nematodes and activities of other microbes during the development of pine-wilt disease in *Pinus thunbergii*. J Jpn For Soc **74:** 383–389

Kuroda K, Kanbara Y, Inoue T, Ogawa A (2006) Magnetic resonance micro-

imaging of xylem sap distribution and necrotic lesions in tree stems. IAWA J **27:** 3–17

Maherali H, Pockman WT, Jackson RB (2004) Adaptive variation in the vulnerability of woody plants to xylem cavitation. Ecology **85:** 2184–2199

Mamiya Y (1975) Behavior of pine wood nematodes in pine wood in early stage of disease development. Trans Mtg Jpn For Soc **86:** 285–286

Mamiya Y (1980) Inoculation of the first year pine (*Pinus densiflora*) seedlings with *Bursaphelenchus lignicolus* and the histopathology of diseased seedlings. J Jpn For Soc **62:** 176–183

Mamiya Y (1985) Initial pathological changes and disease development in pine trees induced by the pine wood nematode, *Bursaphelenchus xylophilus*. Ann Phytopath Soc Jpn **51:** 546–555

Mamiya Y (1990) Behavior of the pine wood nematode, *Bursaphelenchus xylophilus*, and disease development in pine trees. Nippon Nogeikagaku Kaishi **64:** 1243–1246

Nobuchi T, Tominaga T, Futai K, Harada H (1984) Cytological study of pathological changes in Japanese black pine (*Pinus thunbergii*) seedlings after inoculation with pine-wood nematode (*Bursaphelenchus xylophilus*). Bull Kyoto Univ For **56:** 224–233

Odani K, Sasaki S, Nishiyama Y, Yamamoto N (1985) Early symptom development of the pine wilt disease by hydrolytic enzymes produced by the pine wood nematodes: cellulase as a possible candidate of the pathogen. J Jpn For Soc **67:** 366–372

Pittermann J, Sperry JS (2006) Analysis of freeze-thaw embolism in conifers: the interaction between cavitation pressure and tracheid size. Plant Physiol **140:** 374–382

Sasaki S, Odani K, Nishiyama Y, Hayashi Y (1984) Development and recovery of pine wilt disease studied by tracing ascending sap flow marked with water soluble stains. J Jpn For Soc **66:** 141–148

Smith WH (1970) Tree Pathology: A Short Introduction. Academic Press, New York

Sperry JS (1993) Winter xylem embolism and spring recovery in *Betula cordifolia*, *Fagus grandifolia*, *Abies balsamea* and *Picea rubens*. *In* M Borghetti, J Grace, A Raschi, eds, Water Transport in Plants under Climatic Stress. Cambridge University Press, Cambridge, UK, pp 86–98

Sperry JS, Nichols KL, Sullivan JEM, Eastlack SE (1994) Xylem embolism in ring-porous, diffuse-porous, and coniferous trees of northern Utah and interior Alaska. Ecology **75:** 1736–1752

Sperry JS, Sullivan JEM (1992) Xylem embolism in response to freeze-thaw cycles and water stress in ring-porous, diffuse-porous, and conifer species. Plant Physiol **100:** 605–613

Sperry JS, Tyree MT (1988) Mechanism of water stress-induced xylem embolism. Plant Physiol **88:** 581–587

Sperry JS, Tyree MT (1990) Water-stress-induced xylem embolism in three species of conifers. Plant Cell Environ **13:** 427–436

Tamura H (1983) Pathogenicity of aseptic *Bursaphelenchus xylophilus* and associated bacteria to pine seedlings. Jpn J Nematol **13:** 1–5

Tamura H, Yamada T, Mineo K (1988) Host responses and nematode dispersion in *Pinus strobus* and *P. densiflora* infected with the pine wood nematode, *Bursaphelenchus xylophilus*. Ann Phytopath Soc Jpn **54:** 327–331

Tokushige Y, Kiyohara T (1969) *Bursaphelenchus* sp. in the wood of dead pine trees. J Jpn For Soc **51:** 193–195

Tyree MT, Zimmermann MH (2002) Xylem Structure and Ascent of Sap, Ed 2. Springer, Berlin

Utsumi Y, Sano Y, Funada R, Fujikawa S, Ohtani J (1999) The progression of cavitation in earlywood vessels of *Fraxinus mandshurica* var *japonica* during freezing and thawing. Plant Physiol **121:** 897–904

Utsumi Y, Sano Y, Funada R, Ohtani J, Fujikawa S (2003) Seasonal and perennial changes in the distribution of water in the sapwood of conifers in a sub-frigid zone. Plant Physiol **131:** 1826–1833

Utsuzawa S, Fukuda K, Sakaue D (2005) Use of magnetic resonance microscopy for the nondestructive observation of xylem cavitation caused by pine wilt disease. Phytopathology **95:** 737–743

Van As H (2007) Intact plant MRI for the study of cell water relations, membrane permeability, cell-to-cell and long distance water transport. J Exp Bot **58:** 743–756

Windt CW, Vergeldt FJ, de Jager PA, Van As H (2006) MRI of long-distance water transport: a comparison of the phloem and xylem flow characteristics and dynamics in poplar, castor bean, tomato and tobacco. Plant Cell Environ **29:** 1715–1729